Environment International 175 (2023) 107945

Contents lists available at ScienceDirect

Environment International

journal homepage: www.elsevier.com/locate/envint

Full length article

New insights into the combined toxicity of aflatoxin B1 and fumonisin B1 in HepG2 cells using Seahorse respirometry analysis and RNA transcriptome sequencing

Xiangrong Chen [a,*], Mohamed F. Abdallah [a,b], Charlotte Grootaert [a], Filip Van Nieuwerburgh [c], Andreja Rajkovic [a,*]

[a] Department of Food Technology, Safety and Health, Faculty of Bioscience Engineering, Ghent University, Ghent, Belgium
[b] Department of Forensic Medicine and Toxicology, Faculty of Veterinary Medicine, Assiut University, Assiut, Egypt
[c] Laboratory of Pharmaceutical Biotechnology, Faculty of Pharmaceutical Sciences, Ghent University, Ghent, Belgium

ARTICLE INFO

Handling Editor: Adrian Covaci

Keywords:
Aflatoxin B1
Fumonisin B1
Bioenergetics
Seahorse analysis
p53
Mitochondrial toxicity
Apoptosis
Transcriptomics

ABSTRACT

Aflatoxin B1 (AFB1) and fumonisin B1 (FB1) are widely (co-)detected in food and known for their hepatotoxicity in humans. Still, their combined toxicity needs to be investigated, especially the impact on mitochondria. In our previous work, we examined the effect of short-term exposure to different doses of AFB1, FB1, and their binary mixture (MIX) on the bioenergetic status of HepG2 cells, a well-recognized *in vitro* model system for studying liver cell function. In the current work, we further investigated the (combined) effect of AFB1 and FB1 on the mitochondrial and glycolytic activity of HepG2 cells using Seahorse respirometry analysis and RNA transcriptome sequencing. The results showed that the co-exposure, especially at high doses, is more toxic due to a more inhibition of all parameters of mitochondrial respiration. However, FB1 contributes more to the MIX effects than AFB1. RNA transcriptome sequencing showed that the p53 signaling pathway, a major orchestrator of mitochondrial apoptosis, was differentially expressed. Moreover, the co-exposure significantly downregulated the genes encoding for Complexes I, II, III, and IV, representing the onset of the suppressed mitochondrial respiration in HepG2 cells.

1. Introduction

Recent advances in mycotoxin analysis showed that the co-occurrence of several mycotoxins in a single food or edible crop is more common than an individual mycotoxin (Palumbo et al., 2020). However, most of the available knowledge regarding the toxicity of mycotoxins in human is limited to the study of a single mycotoxin, and little is known about the interaction of a mycotoxin mixture in the biological systems. Such interaction could be additive, antagonistic, or synergistic, which may alter the toxic outcomes (Alam et al., 2022). Currently, the number of mycotoxins in food is expected to be much more than 400, varying in their chemical structures and hence their toxicities (Decleer et al., 2018; Palumbo et al., 2020; Wu et al., 2014). In the present work, we have selected two mycotoxins (aflatoxin B1 and fumonisin B1) which have been found to co-occur in different food samples, especially maize, collected from Africa, America, Asia, and Europe (Chen et al., 2021; Du et al., 2017; Palumbo et al., 2020). Aflatoxin B1 (AFB1) and fumonisin B1 (FB1) are among the most toxic fungal secondary metabolites. The International Agency for Research on Cancer (IARC) classified AFB1 as a group 1 carcinogen due to the sufficient evidence of causing liver cancer in humans, while FB1 is classified as a class 2B carcinogen as the evidence of causing cancer is limited (IARC, 2012). Other toxic effects of AFB1 and FB1 also include hepatotoxicity, nephrotoxicity, and embryotoxicity, immunotoxicity (Chen et al., 2022; Wang et al., 2022).

Mitochondria are critical cellular organelles that make adenosine triphosphate (ATP) appropriately in response to cellular energy demands, hence known as the powerhouse of the cell (Vyas et al., 2016). Besides, these organelles perform many roles, including generating reactive oxygen species (ROS) and regulating cell signaling. Due to their high abundance in hepatocytes, they have been recognized as a critical mediator in hepatotoxicity. Such toxicity could be induced by the loss of mitochondrial function, creating a mitochondrial metabolic gridlock, such as the inhibition of mitochondrial respiration (Prakash et al.,

* Corresponding authors.
E-mail addresses: xiangrong.chen@ugent.be (X. Chen), andreja.rajkovic@ugent.be (A. Rajkovic).

https://doi.org/10.1016/j.envint.2023.107945
Received 2 February 2023; Received in revised form 8 April 2023; Accepted 19 April 2023
Available online 24 April 2023

2022). The *in vitro* hepatotoxicity of AFB1 and FB1 has been reported in many studies using the HepG2 cells as the preferred liver model (Abdul and Chuturgoon, 2021; Chen et al., 2022; Singto et al., 2020). Oxidative stress, inflammation, and mitochondrial dysfunction by targeting ROS, DNA, p53, and other signaling pathways have been documented as toxic mechanisms of AFB1 (Li et al., 2022). Similarly, FB1 has been reported to induce hepatotoxicity by inhibiting sphingolipids biosynthesis and triggering massive production of ROS (Sheik Abdul and Marnewick, 2020).

Based on these studies, it has been found that both AFB1 and FB1 could damage mitochondrial function to cause hepatotoxicity. Currently, there are few reports on the use of *in vitro* systems for the analysis of AFB1 and FB1 mixtures, especially the effect on mitochondria. Therefore, purpose of the current study aimed at investigating the impact of AFB1 and FB1 as well as their combination (binary mixture) on the mitochondrial and glycolytic activities. This has been performed using Seahorse Extracellular Flux Analysis to decipher the bioenergetic phenotype, and RNA sequencing (Illumina) to better understand functional biology underlying the observed phenotypic mitochondrial function signatures.

2. Materials and methods

2.1. Chemical reagents

The mycotoxin FB1 (Cas. No. 116355-83-0; 99% purity) was obtained from Sigma (USA), while AFB1 (Cas. ALX-630-093-M005; >98% purity) was purchased from Enzo Life Sciences (Belgium). Stock solutions (10 mg/mL) of FB1 and AFB1 were prepared in dimethyl sulfoxide (DMSO) and stored at −20 °C, and working solutions were freshly prepared in a cell growth medium at different concentrations and combinations of FB1 and AFB1 (Table 1). It is important to mention that due to the carcinogenic properties of AFB1 in humans, it is essential to implement stringent safety measures when handling this compound for experimental purposes. Phosphate buffer saline (PBS) with and without Ca^{2+} and Mg^{2+} were obtained from Westburg (Leusden, Netherlands).

2.2. Cell culture and mycotoxin exposure

HepG2 cells (derived from human hepatocellular carcinoma) were obtained from the American Type Culture Collection (ATCC, Manassas, VA, USA) and cultured as described in the literature (Chen et al., 2022). The cells were exposed to three different concentrations of AFB1 (0.5, 2, and 8 μg/mL) and FB1 (10, 40, and 160 μg/mL) to mimic three different scenarios of exposure (low, middle, and high). Furthermore, three combinations (low-low, middle-middle, and high-high) as a binary mixture (MIX) of AFB1 and FB1 were prepared (Table 1). These concentrations were selected based on the estimated exposure data derived from calculating the average of urinary biomarkers of AFB1 (0.5 μg/mL) and FB1(10 μg/mL) in humans, which were considered as low exposure scenario in this study (Chen et al., 2022; Meneely et al., 2018). This low exposure scenario was increased four-folds to represent a middle exposure scenario and sixteen-folds to represent a high exposure scenario to assess potential toxicity.

Table 1
Different concentrations of AFB1 and FB1, alone and in combination, used in the current study.

Concentrations	AFB1 (μg/mL)	FB1 (μg/mL)	MIX	
			AFB1 (μg/mL)	FB1 (μg/mL)
Low	0.5	10	0.5	10
Middle	2	40	2	40
High	8	160	8	160

2.3. Cytotoxicity endpoint measurements (MTT, ROS, and MMP)

The tetrazolium salt (MTT) assay was performed to determine the cell viability after exposure to AFB1 and FB1 (Chen et al., 2022). ROS and MMP (mitochondrial membrane potential) were measured to reflect the cytotoxic effect of AFB1 and FB1 in HepG2 cells. The applied toxic doses of AFB1, FB1, and their mixture (MIX) are shown in Table 1. These three assays were measured using SpectraMax™ Microplate Reader (Molecular Devices, Berkshire, UK), as described in the literature (Chen et al., 2022).

2.4. HepG2 bioenergetic analysis using Seahorse Extracellular Flux Analyzer (total ATP production, glycolysis, and mitochondrial respiration)

The Seahorse XF96 Analyzer instrument (Agilent Seahorse Bioscience, CA, USA) and the related consumables (plates, cartridges, and inhibitor kits) were used to measure total ATP production, glycolysis, and mitochondrial respiration according to the manufacturer's instructions. In brief, the assay medium was prepared by supplementing Seahorse XF Base medium (pH 7.4) with a specific combination of ten mM glucose (100X stock, Agilent), one mM pyruvate (100X stock, Agilent), and two mM L-glutamine (Sigma). At first, cells were harvested and seeded into a Seahorse 96-well XF Cell Culture microplate in 80 μL of the culture medium (20,000 cells/well). The optimal cell density was previously determined and is part of laboratory SOPs for different cell types. The cells were incubated at 37 °C in a pre-sterilized incubator with an atmosphere containing 10% CO_2 and 95% constant humidity for 24 h. Next, HepG2 cells were treated with the same doses of AFB1, FB1, and MIX, as shown in Table 1.

In parallel, a Seahorse XF Sensor Cartridge was hydrated 24 h before running the XF Assay by filling each well of the XF Utility Plate with 200 μL of sterile water. On the analysis day, the sterile water was replaced by Seahorse XF calibrant solution. The hydrated cartridge was for 24 h maintained in an incubator at 37 °C without CO_2 to remove CO_2 from the media that may interfere with measurements by altering the pH. Cell washing and measurement cycles were performed following our established protocol (Chen et al., 2022). The preformulated and optimized Seahorse-specific real-time ATP rate assay kit, glycolysis stress test kit and Mito stress test kit (all from Agilent) were used to measure total ATP production, glycolysis, and mitochondrial respiration, respectively. The accurate concentrations and volumes for each inhibiting compound used in each kit are described in Table 2. Seahorse Wave Controller Software version 2.6.3 (Agilent Seahorse Bioscience, CA, USA) was used to operate and control the Seahorse XF96 Analyzer instrument. After the measurements were done, data were exported for processing and analysis (see **Data processing and analysis**). Normalization was performed

Table 2
Required concentrations and volumes of each inhibitor per assay.

Kit		Agilent Seahorse XF real-time ATP rate assay kit	Agilent Seahorse XF glycolysis stress test kit	Agilent Seahorse XF cell mito stress test kit
Port A	Compound (S)	Oligomycin	Glucose	Oligomycin
	Concentration (μM)	1.5	10,000	1
	Volume (μL)	20	20	20
Port B	Compound (S)	Rotenone Antimycin A	Oligomycin	FCCP
	Concentration (μM)	0.5	1	0.25
	Volume (μL)	22	22	22
Port C	Compound (S)	–	2-Deoxy-D-glucose (2-DG)	Rotenone Antimycin A
	Concentration (μM)	–	50,000	0.5
	Volume (μL)	–	25	25

by fixing the cells using sulforhodamine B dye (Sigma-Aldrich, Co., St. Louis, MO, USA) as described before (Chen et al., 2022).

2.5. Transcriptome analysis (RNA isolation, processing, and sequencing)

The complete set of RNA transcripts from HepG2 was studied at high concentrations of AFB1 (8 μg/mL) and FB1 (160 μg/mL), as well as their binary combination (high MIX), since these concentrations and combination induced toxic effect on mitochondria according to the Seahorse Extracellular Flux Analysis. Transcriptome analysis, including RNA isolation, processing, and sequencing, was conducted according to established protocols (Degroote et al., 2021). The experiment was repeated independently five times with identical conditions to provide at least five biological replicates for each time point and treatment. In summary, HepG2 cells were cultivated in six well-plate at the same cell density. After 24 h of exposure to the mycotoxins, the growth media were completely removed. To harvest the cells, one mL of PBS was added to each well, and the adherent cells were collected by cell scrapers (Greiner Bio-One, Vilvoorde, Belgium) and transferred into two mL Eppendorf tubes. After centrifugation for two minutes at 8000 g, the supernatant was discarded, and the RNA extraction was performed with the RNeasy® Mini Kit (Qiagen, Hilden, Germany) following the instruction handbook. In short, 600 μL lysis Buffer RLT was applied to the pellets, 600 μL of 70% ethanol was added, and the total volume was transferred to an RNeasy Mini spin column placed in a collection tube to be centrifuged at 8000 g for 15 s. The flow-through was discarded, and the column was washed with Buffer RW1 and Buffer RPE before eluting the RNA in 40 μL RNase-free water. A Bioanalyzer RNA 6000 Nano assay (Agilent Technologies, CA, USA) was used to measure the RNA quality, providing a RIN (RNA Integrity Number) value. All the samples had an RNA integrity number (RIN) value above nine. RNA from each sample was quantified using the 'Quant-it ribogreen RNA assay' (Life Technologies, Grand Island, NE, USA), and 500 ng RNA was used to prepare an Illumina sequencing library using the QuantSeq 30 mRNA-Seq Library Prep Kit (Lexogen, Vienna, Austria) according to manufacturer's protocol with 14 enrichment polymerase chain reaction (PCR) cycles. An average of $9.0 \times 10^6 \pm 1.8 \times 10^6$ and $11.6 \times 10^6 \pm 1.0 \times 10^6$ reads were generated.

2.6. Data processing and analysis

The SPSS software (SPSS Statistics 27, USA) was used for the statistical evaluation. Comparisons between the untreated control and different FB1 and AFB1 treatments within each mitochondrial parameter were performed using a one-way analysis of variance (ANOVA) test, followed by Tukey HSD multiple-comparison test as a post hoc analysis to identify the sources of detected significance ($p < 0.05$). The data are presented as mean ± standard deviation (SD). Analysis for differential gene expression was performed using the edgeR's (40) quasi-likelihood method between two conditions, only including genes expressed at a counts-per-million (cpm) above one in at least five samples. Genes were considered significantly differential if they had a false discovery rate (FDR) < 0.05 and a fold change of at least 2. Gene set enrichment analysis (GSEA) was performed using the GAGE R package, based on the Kyoto encyclopedia of genes and genomes (KEGG) pathways provided by this package. Genes and KEGG pathways of interest were selected based on their impact on diabetes pathology, hepatic fat synthesis, and energy metabolism. Significance thresholds $|\log(FC)| > 1$ and FDR < 0.05 were set in performing heatmaps; $|\log2FC| = 1$ and $P = 0.05$ were set in performing volcano plots based on edgeR analysis. Finally, the effects of mycotoxins (AFB1, FB1 and their mixture) on pathways were also calculated and displayed in the heat map. The heat map expresses the magnitude enrichment analysis was performed using the GSEA software (v4.2.3) and Molecular Signatures Database (MSigDB) Hallmark Gene Signatures. Gene sets were considered significantly enriched when q-value FDR < 0.05, and normalized enrichment scores (NES) were used for further calculations, such as z-scores.

3. Results

3.1. Cytotoxicity of AFB1, FB1, and their combination after measuring MTT, ROS, and MMP

Treatment of HepG2 cells with either AFB1 or FB1 or their binary combination (MIX), resulted in a concentration-dependent increase in intracellular ROS and induction of MMP disruption. As shown in Fig. 1, a combination of AFB1 and FB1 at low concentration (low MIX) did not have inhibitory effects on cellular viability compared to the individual effect imposed by either AFB1 or FB1 treatment. While a binary mixture of AFB1 and FB1 at middle and high concentrations (middle and high

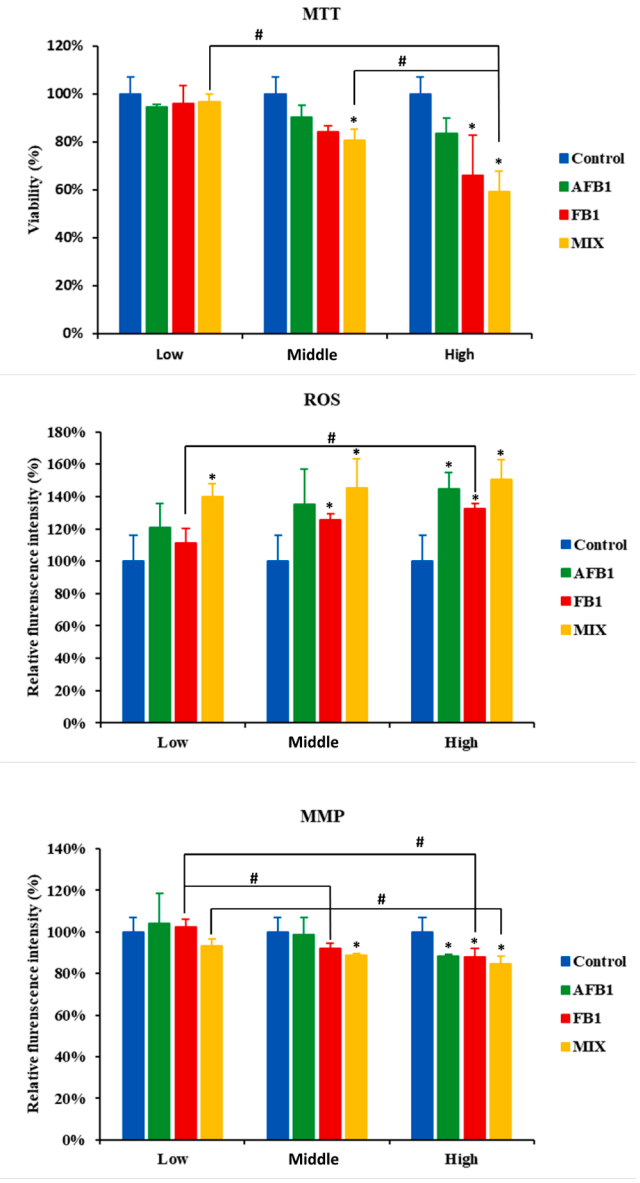

Fig. 1. Effect of FB1, AFB1, and MIX on cell viability (MTT), intracellular reactive oxygen species (ROS), and mitochondrial membrane permeability (MMP) in HepG2 cells after 24 h exposure. Data (at least three well-replicates) are expressed as mean ± standard deviation. Significance compared to the mycotoxin-free condition is labeled by *: $p < 0.05$ according to a one-way ANOVA with Dunnett's post hoc test. Significance compared to the same mycotoxin per concentration is labeled by #: $p < 0.05$ according to the one-way ANOVA with Tukey HSD multiple-comparison post hoc test.

MIX) led to a significant loss of cell viability, which was between 9 and 24% and 3–7% higher compared to the loss of cell viability caused by AFB1 and FB1 alone, respectively. Significant increases in intracellular ROS levels were detected in case of exposure to AFB1 (high concentration) and FB1 (middle and high concentration) as well as the three levels of combinations (low, middle, and high MIX). The increase in ROS levels with a combination (MIX) was between 5 and 19% higher than the ROS levels with AFB1 and between 18 and 29% higher than those levels detected with FB1. As depicted in Fig. 1, the MMP disruption in HepG2 cells exposed to high concentrations of AFB1 (8 μg/mL) and FB1 (160 μg/mL), as well as their binary combination (high MIX) showed a slight but significant ($p < 0.05$) dose-dependent MMP decrease. This decrease in MMP levels was about 12% for AFB1 and FB1 alone, and about 16% for the MIX, compared to the MMP from the untreated control cells. These results demonstrate that the applied doses of AFB1 and FB1 reduce cell viability and MMP and induce the generation of more intracellular ROS in HepG2 cells. By comparing the toxic impact of AFB1 or FB1 and their MIX in each exposure scenario (low, middle, and high), the binary combination (MIX) shows a trend of more potent effects in all cytotoxicity endpoints. However, this did not always show statistically significant differences compared to the effect caused by AFB1 or FB1 alone.

3.2. Impact of AFB1, FB1 and their combination on HepG2 bioenergetics

3.2.1. Total ATP production

To investigate the impact of AFB1, FB1 and their combination on the total ATP production derived from glycolysis and mitochondrial respiration via oxidative phosphorylation (OXPHOS), the Seahorse XF Real-Time ATP Rate assay was used. As depicted in Fig. 2, the total ATP production was inhibited in the three scenarios of exposure (low, middle, and high) either after individual treatment with AFB1 or FB1 or their binary combination (MIX) in a concentration-dependent manner. These inhibitions were statistically significant ($p < 0.05$) compared to the untreated control, except for the FB1 at low dose. Interestingly, the exposure to AFB1 or FB1 or their combination (MIX) at the highest levels of exposure significantly shifted the balance or the contribution ratio of glycolysis versus OXPHOS for the total ATP yield to be more relying on the ATP generation via OXPHOS. After the exposure to MIX (low and middle level), the inhibition of the ATP production is situated between the effects of the single toxin treatments, thereby suggesting interactions at the energy-providing pathway level. In contrast, upon exposure to high MIX, it showed the most substantial decrease (but not significant compared the individual exposure to toxins) in total ATP production and caused a significant shift compared to the AFB1 and FB1 condition(s) from glycolytic to mitochondrial ATP production of 34% that is the difference of OXPHOS ATP (67%) and glycolysis (33%). In several cancer cells, such as HepG2 cells, glycolysis is enhanced, and OXPHOS capacity is diminished. In the current work, the observed shifts in the contribution ratio between the glycolysis and OXPHOS for the total ATP provide an unfavorable environment for cell growth (Zheng, 2012).

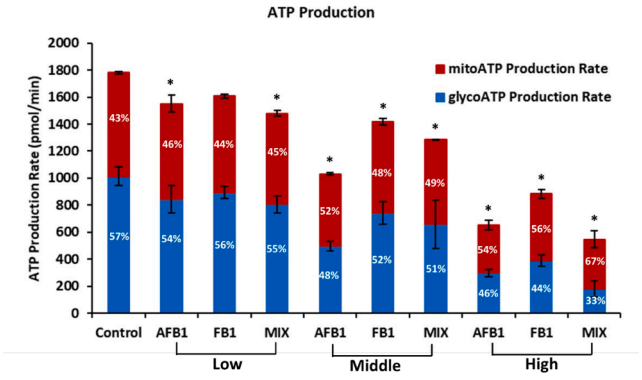

Fig. 2. Effect of AFB1, FB1, and MIX on mitochondrial and glycolytic ATP production rates in HepG2 cells after 24 h exposure. Data (at least four technical replicates) are expressed as mean ± standard deviation. *: $p < 0.05$ indicates significantly different results compared to the untreated condition control by the one-way ANOVA with Dunnett's post hoc test.

3.2.2. Glycolytic pathway for energy production in HepG2 cells

The glucose is converted into pyruvate (referred to as glycolysis), which results in the net production and extrusion of protons into the extracellular medium. The Extracellular Acidification Rate (ECAR) is related to the lactate secretion, which is directly related to the glycolytic flux. Therefore, the glycolytic activity of HepG2 was determined following real-time changes in ECAR levels by measuring four different parameters (glycolysis, glycolytic capacity, glycolytic reserve and non-glycolytic acidification) using the Seahorse XF96 Analyzer. At low exposure level, only the glycolysis and glycolytic capacity in case of AFB1 and the glycolysis in case of the MIX (AFB1 and FB1) were significantly reduced (Fig. 3). After a 24 h of exposure to middle or high doses with either AFB1 or FB1 or their binary combination (MIX), a significant reduction ($p < 0.05$) in the glycolysis, glycolytic capacity, and nonglycolytic acidification parameters were observed. Although the exposure to combination of the two toxins (especially at high MIX) showed more inhibitory effect compared to the individual treatment (AFB1 or FB1), these decreases were not statistically significant. These results demonstrate that high MIX (8 μg/mL for AFB1 and 160 μg/mL for FB1) might have a more disruptive effect on glycolysis. However, the significant interaction of AFB1 and FB1 on the negative impact on glycolytic activity was not observed. On the other hand, in all the three exposure scenarios, AFB1 or FB1 or their binary combination did not affect the glycolytic reserve of HepG2 with the exception of the high dose of AFB1 (Fig. 3).

3.2.3. Mitochondrial respiration pathway for energy production in HepG2 cells

In parallel, the effect of AFB1 and FB1 mixture on the ability of HepG2 cells to regulate mitochondrial respiration compared to the single exposure to AFB1 or FB1 was examined. In this regard, Oxygen Consumption Rate (OCR) is used as an indicator of mitochondrial respiration. Inhibition was observed in the mitochondrial activity of HepG2 cells after exposure to three levels (low, middle, and high) of AFB1 or FB1 or their combination (MIX) (Fig. 4). Especially the exposure to AFB1 or FB1 or their binary combination (MIX) at high levels of exposure decreased the basal respiration, maximal respiration, ATP production, and proton leak ($p < 0.05$) and increased the spare respiratory capacity ($p < 0.05$) compared to untreated control. Moreover, when HepG2 cells were exposed to a combination of the two toxins (high MIX), all these mitochondrial parameters were significantly decreased in comparison to the individual treatment of high AFB1 (8 μg/mL) or high FB1 (160 μg/mL). However, these significant decreases were not always present in the other two exposure scenarios (low and middle) between comparisons of the individually toxic impact of AFB1 or FB1 with their binary combination (MIX). These results demonstrate that high MIX (8 μg/mL for AFB1 and 160 μg/mL for FB1) might cause more disruption of the mitochondrial metabolism, and significant changes in mitochondrial dysfunction seem to be attributed to the toxic the interaction between AFB1 and FB1.

3.3. Impact of AFB1, FB1 and their combination on HepG2 transcriptomic responses

3.3.1. Expression profiles of mRNAs in experimental groups

A total number of 29,744 genes were detected after the exposure of HepG2 cells to either AFB1 (8 μg/mL) or FB1 (160 μg/mL) or their binary combination (MIX: 8 μg/mL for AFB1 and 160 μg/mL for FB1). A heatmap based on the color key for the gene clustering is depicted in

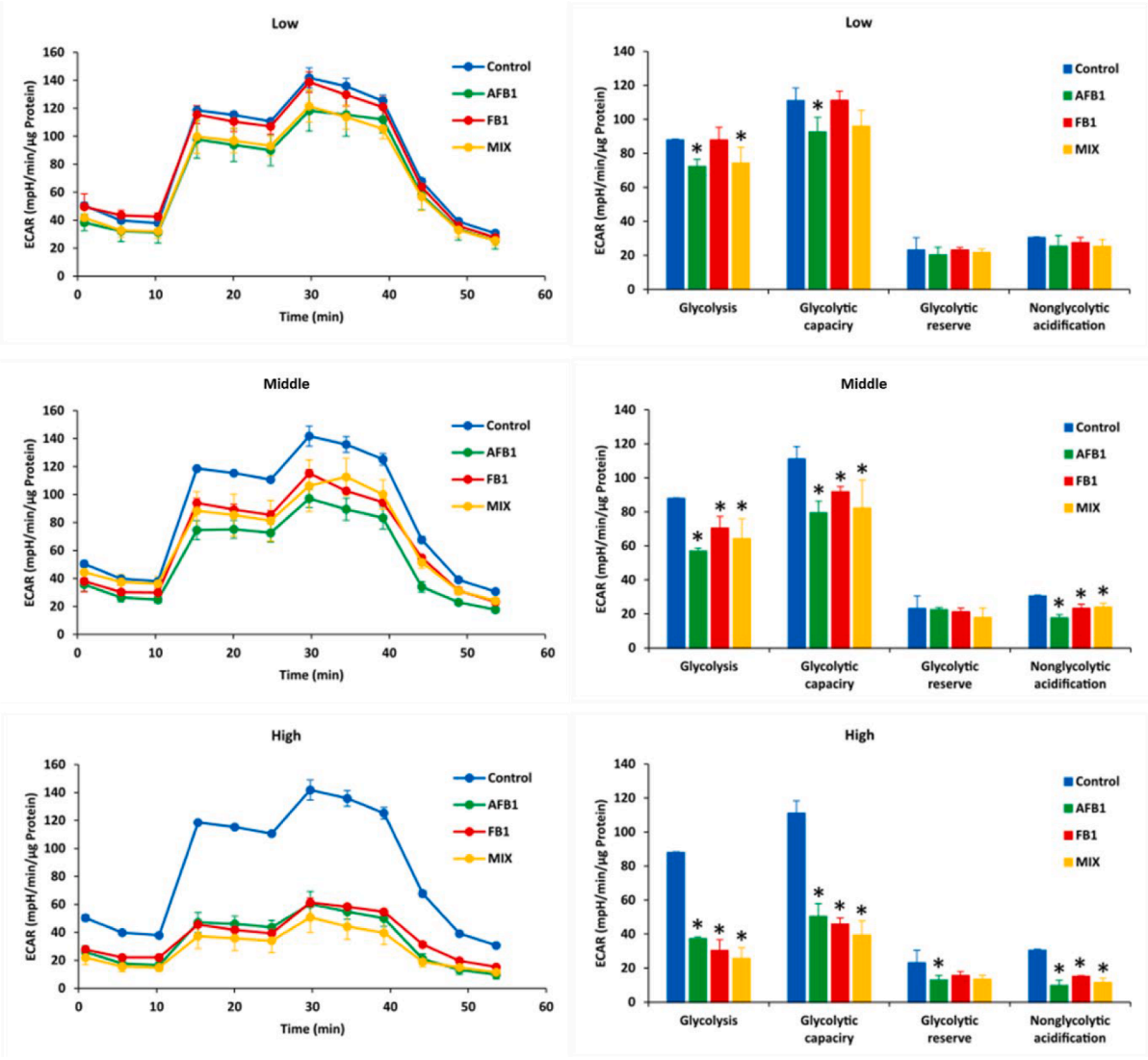

Fig. 3. Effect of AFB1, FB1, and MIX on extracellular acidification rate (ECAR) (left) and different glycolytic parameters (right) in HepG2 cells after 24 h exposure. Data (at least four technical replicates) are expressed as mean ± standard deviation. Mean values with different symbols (*: compared to control) within each glycolytic parameter indicate significant differences ($p < 0.05$) among other treatments according to the one-way ANOVA test followed by the Tukey HSD multiple-comparison test as a post-doc analysis.

Fig. 5**a**. Replicates from the same condition always cluster together, generating four clusters according to HepG2 cell treatments. Regardless of the treatment condition, the untreated control group was distinctly separated. The FB1 and MIX groups clustered together, indicating a solid contribution of FB1 to the overall MIX effect compared to AFB1 alone, which yielded a clearly distinct expression pattern compared to the other conditions (Fig. 5**a**). A volcano plot based on the log Fold Change (FC) and the False Discovery Rate (FDR) of each tested gene is shown in Fig. 5**b**. The cutoff value for the FDR was adjusted at 0.05, while log2FC < -1 for the downregulated genes and log2FC > 1 for upregulated genes were set to check the top significant genes. Compared to the MIX group, AFB1-treated samples showed several downregulated genes (in the blue color) and upregulated genes (in the red color). On the other hand, the FB1-treated group had fewer fold changes in the expressed gene compared to the MIX group (i.e., fewer significant genes). The Venn diagrams in Fig. 5**c** show the differential genes that were either upregulated or downregulated between the treatments. Compared to the untreated control (CON), AFB1 resulted in 2336 differentially expressed genes (DEGs), of which 558 DEGs were identical to those differentially expressed upon MIX treatment, which contained 312 upregulated DEGs and 246 downregulated DEGs. Similarly, compared to CON, FB1 treatment resulted in 2321 DEGs, of which 1318 DEGs were identical to those differentially expressed upon MIX treatment, including 609 upregulated DEGs and 709 downregulated DEGs. Compared to the MIX condition, only 72 upregulated and 10 downregulated DEGs were shared between AFB1 and FB1, thereby confirming the different mode-of-action of both mycotoxins. In these Venn diagrams, it is also clearly visible that the single AFB1 condition is more distinct than the FB1 and thus contributes less to the MIX effects.

3.3.2. Kyoto encyclopedia of genes and genomes (KEGG) analysis-p53 pathway

Pathway analysis based on Gene Ontology (GO) (50 pathways) and Kyoto Encyclopedia of Genes and Genomes (KEGG) (338 pathways) databases led to the discovery of significantly enriched pathways upon AFB1 and FB1 treatment versus a combination of the two mycotoxins (MIX) treatment. The KEGG analysis identified six significantly different KEGG pathways (Herpes simplex virus one infection, Ribosome, Fanconi anemia pathway, Amyotrophic lateral sclerosis, Cell cycle, and p53 signaling pathway) when comparing FB1 and MIX. In contrast, no

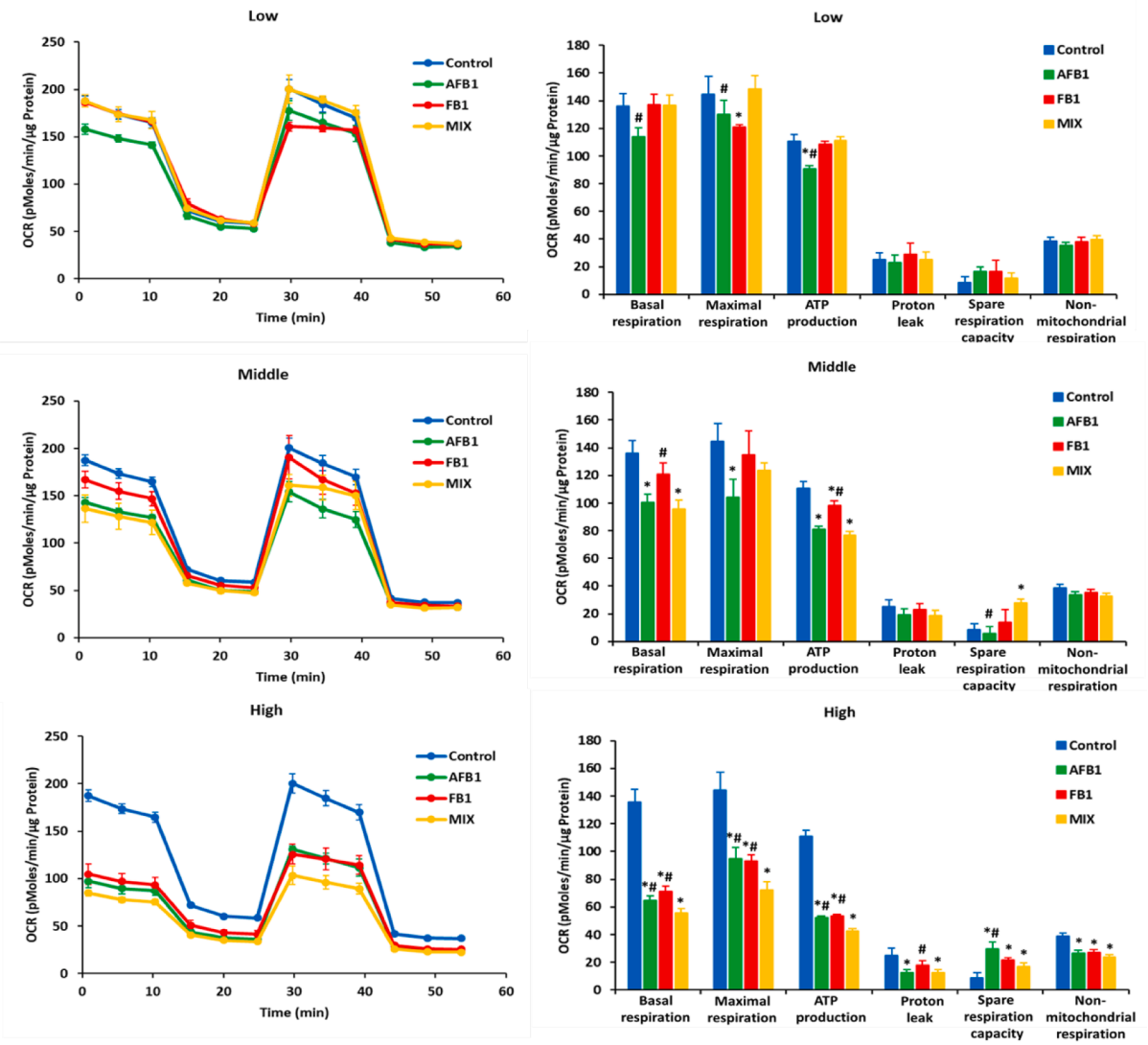

Fig. 4. Effect of AFB1, FB1, and MIX on oxygen consumption rate (OCR) (left) and different mitochondrial parameters (right) in HepG2 cells after 24 h exposure. Data (at least four technical replicates) are expressed as mean ± standard deviation. Mean values with different symbols (*: compared to control; #: compared to MIX) within each mitochondrial parameter indicate significant differences ($p < 0.05$) among other treatments according to the one-way ANOVA test followed by the Tukey HSD multiple-comparison test as a post hoc analysis.

differential pathways were identified between AFB1 and MIX. Overall these pathways, the p53 signaling pathway is actively involved in bioenergetics and cell death. Fig. 6 shows the p53 signaling pathway genes that are differentially expressed with the comparison of FB1 and MIX. In this signaling pathway, MIX significantly downregulated Fas, DR5, Nora, PUMA, PIGs, Pag608, and upregulated p53, Bcl-xL, and Scotin. Subsequently, genes with mitochondrial and hence bioenergetic impact were significantly downregulated by MIX, including Cx I, Cx II, Cx III, Cx IV, PINK, and Bad. Cx I, Cx II, Cx III, and Cx IV are central mitochondria respiratory complexes in the electron transport chain (ETC) linked to the CytC-inducing apoptosis. As a result, further downregulated CytC, Apaf-a, CASP9, and CASP3, which may explain the cell death, possibly mediated by apoptosis in HepG2 cells. Because these differences were seen at the whole pathway level, there is strong evidence that they pinpoint the primary mode of action explaining the previous results.

3.3.3. Gene ontology (GO) analysis

Gene Set Enrichment Analysis (GSEA) using the Hallmark gene sets showed that AFB1, FB1, and their binary combination (MIX) treatments affect critical cellular processes. Key regulatory pathways (such as hypoxia, unfolded protein response, and p53 pathway), metabolic mechanisms (such as cholesterol homeostasis, OXPHOS, and glycolysis), and immune responses (such as TNF-α signaling via NF-κB, mTORC1 signaling, IFN-γ, IFN-α, and inflammatory response) were enriched in AFB1, FB1, and MIX versus CON, as well as in AFB1 and FB1 versus MIX. A heat map of z-scores of the Normalized Enrichment Score (NES) for each hallmark represents the differences in the enrichment of each hallmark between the pre-treatments (Fig. 7). Upon GO analysis, seven differential pathways were identified when comparing FB1 and MIX (UV response DN, E2F targets, G2M checkpoint, p53 pathway, MYC targets V1, DNA repair, and mTORC1 signaling), and four differential pathways when comparing AFB1 and MIX (p53 pathway, MYC targets V2, DNA repair, and UV response DN). It was observed that AFB1 and FB1 mainly disrupted cell proliferation, and as a result, MIX significantly altered proliferation genes compared to CON/AFB1/FB1. In addition, AFB1 also showed significant induction of DNA damage.

4. Discussion

The aim of the current study was to identify the short-term effect of (combined) exposure of AFB1 and FB1 on the cellular energy profiles, including glycolysis and mitochondrial respiration pathways, in HepG2

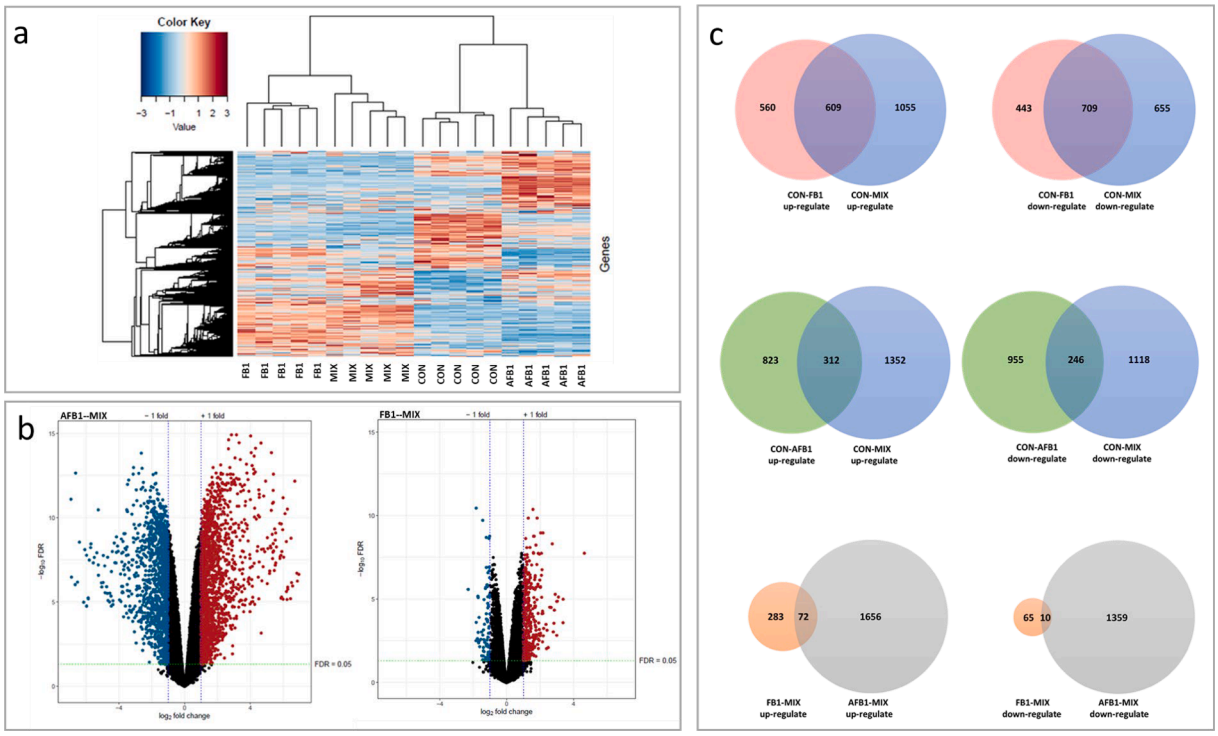

Fig. 5. Differentially expressed genes in experimental groups. (a) Heatmap for outcoming of the weighted gene co-expression network analysis (WGCNA) on all conditions; (b) Volcano plot based on the fold change and the false discovery rate (FDR) of each tested gene. The cutoff for FDR was set at 0.05. Blue dots represent downregulated genes (log2FC < -1), red dots represent upregulated genes (log2FC > 1), black dots represent the genes that did not pass the thresholds for FDR and Log Fold Change; (c) Venn diagrams of the overlapping and different differentially expressed genes (DEGs). (For interpretation of the references to color in this figure legend, the reader is referred to the web version of this article.)

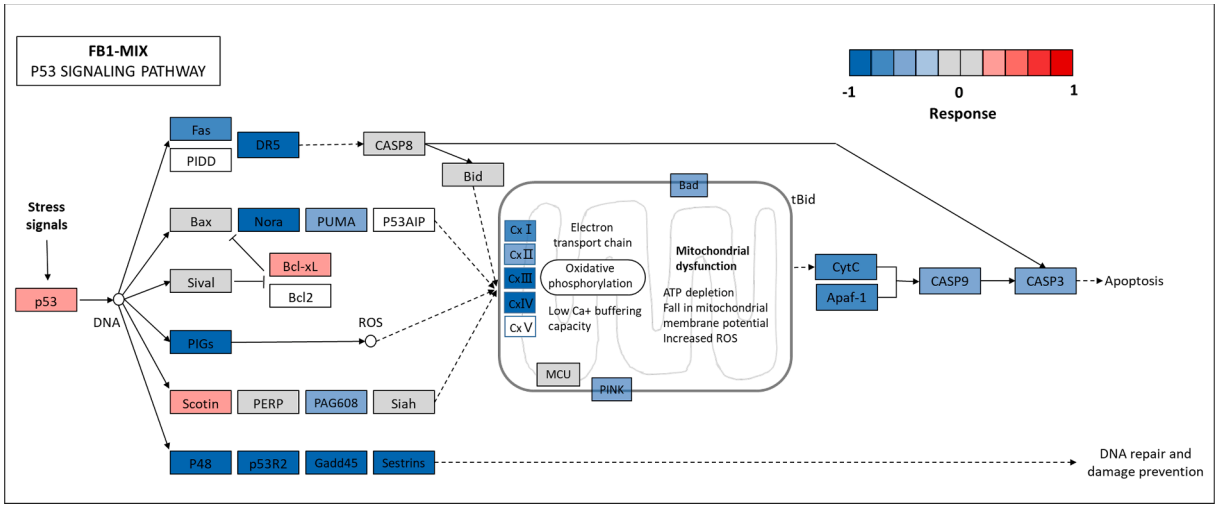

Fig. 6. A pathway diagram of the p53 pathway of FB1-MIX as annotated by the Kyoto Encyclopedia of Genes and Genomes (KEGG). The color in which the genes are marked correlates to the response value of the comparison between fumonisin FB1 (FB1) and the AFB1-FB1 mixture (MIX).

cells. This was accomplished by applying relevant doses and combinations of both mycotoxins, where the low level of exposure or treatment matched with average urinary biomarkers of AFB1 (0.5 μg/mL) and FB1 (10 μg/mL) in humans (Meneely et al., 2018). Two additional levels of exposure were applied by increasing the dose four-folds to have a middle exposure scenario and sixteen-folds to a high exposure scenario to investigate the potential toxicity. It was found that with advanced respirometry techniques revealed differential effects between a single mycotoxin treatment compared to the binary mixture in multiple mitochondrial parameters. Finally, transcriptomics clearly showed different results among all other treatments, and differential pathways and genes revealed a particular focus on mitochondrial and proliferation-related mechanisms.

4.1. Conventional assays confirm earlier findings on cytotoxicity, oxidative stress, and mitochondrial membrane potential

AFB1, FB1, and their binary mixture (MIX) individually caused cytotoxic effects, ROS generation, and MMP disruption in HepG2 cells, and MIX showed a higher toxic effect for these cytotoxicity endpoints. It

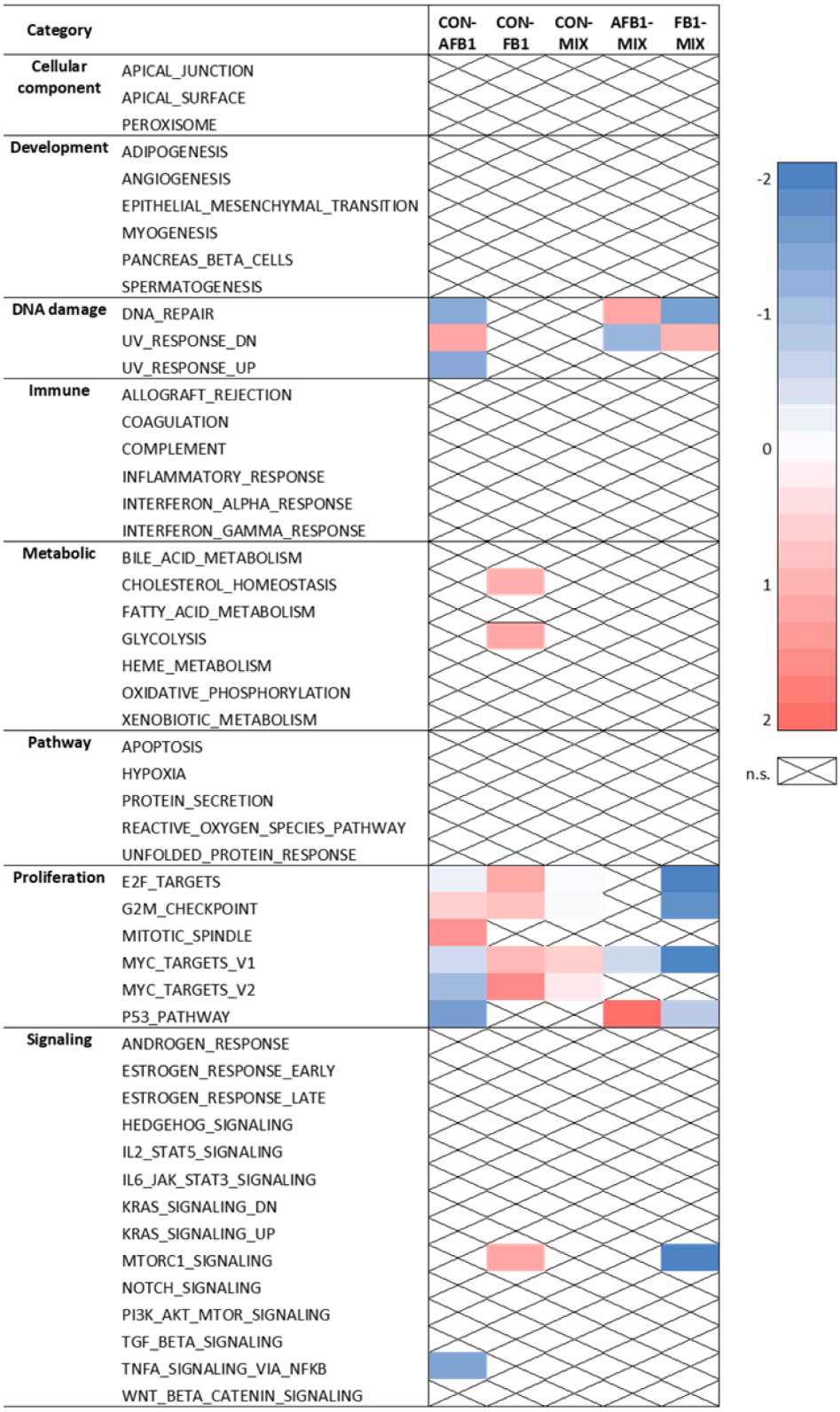

Fig. 7. Heatmap of Z-scores of the MSigDB hallmark gene sets using Gene Set Enrichment Analysis (GSEA), showing the significantly enriched gene sets (FDR < 0.05) across the treatments according to a pairwise comparison. Non-significant (n.s.) differences are marked by X.

is presumed that MIX may aggravate mitochondrial dysfunction, resulting in an increase in ROS generation and induction in MMP disruption. Previous research has elucidated that mitochondrial respiration involves the tricarboxylic acid (TCA) cycle and fatty acid β-oxidation, which generate electrons, and then the electron donors are used by ETC complexes and ATP synthase to carry out oxidative phosphorylation (Vyas et al., 2016). MMP and ROS are generated by proton pumps (complexes) through ETC (Feissner et al., 2009; Zorova et al., 2018). However, when comparing the effects of AFB1/FB1 and MIX in each applied condition, the MIX did not significantly modify cytotoxicity

endpoints (ROS and MMP) compared to the individual toxins, which may be due to the different cytotoxicity-related mode-of-action of AFB1 and FB1 in HepG2 cells. Around 95% of AFB1 would be transformed to AFB1-exo28,9-epoxide (AFBO) in the liver, and the indirect genotoxicity of AFB1 is responsible (probably among other causes) for AFBO. The AFBO could produce direct genotoxicity and ROS induction by forming adducts with the DNA (Zhu et al., 2021). This mode of action was confirmed with the transcriptomics outcomes, in which AFB1-containing treatments involve DNA damage pathways. On the other hand, FB1 could cause liver toxicity, and the most recognized mechanism of action is the disruption of sphingolipid metabolism by inhibiting the ceramide synthase enzyme (Abdul and Chuturgoon, 2021).

4.2. Respirometry reveals interactions between AFB1 and FB1 on mitochondrial dysfunction

To investigate whether the biological processes such as total ATP production, glycolytic and mitochondrial function are affected by the AFB1/FB1 and MIX, their cellular rates were analyzed using the Seahorse XF96 instrument. Glycolysis and OXPHOS are the primary metabolic routes that provide energy to the cell by breaking down nutrients such as glucose, amino acids, and fatty acids to produce ATP (Fox et al., 2005). The Seahorse XF Real-Time ATP Rate Assay allows the calculation of the mitochondrial and glycolytic ATP production rates, providing a new dynamic and quantitative insight into cellular bioenergetics by providing a real-time measurement of oxygen production as a proxy for respiration and lactate secretion as a proxy for glycolysis. The Seahorse XF Glycolysis Stress Test and Mitochondrial Stress Test protocols dissect the glycolytic and respiratory fluxes components into basal, maximal, and reserve (spare) glycolytic or respiratory capacity through the consecutive addition of certain stressors such as oligomycin, FCCP, and rotenone in HepG2 cells. The outcomes of these tests are depicted in Figs. 2, 3, and 4.

AFB1, FB1, and MIX individually disrupted ATP production from glycolysis and mitochondrial respiration or OXPHOS, which is consistent with the cytotoxicity data. Interestingly, the MIX condition showed a greater interference with total ATP production metabolism in HepG2 cells compared to the single mycotoxin treatments. In addition, MIX shifted the fraction of ATP production between OXPHOS and glycolysis from 43%/57% to 67%/33% under high conditions, indicating a particular decrease in glycolysis. Generally, cellular metabolism consumes energy, of which OXPHOS supplies 70%, although cell type-dependent differences are reported (Zheng, 2012). As HepG2 cells have a cancer-derived origin, energy metabolism and glucose and glutamine uptake differ from normal tissues and display a high rate of glycolysis (Zheng, 2012). Due to their different origin and differentiation, glycolysis contributes to most of ATP but does not generally exceed 50–60% in cancer cells (Zu and Guppy, 2004). Therefore, according to our data, it is inferred that combined AFB1 and FB1 could suppress energy metabolism and change metabolic phenotype to adapt to microenvironmental changes, which may result in a selective advantage for HepG2 cells to survive under an unfavorable environment (Marusyk and Polyak, 2010). During cell proliferation, the pentose phosphate pathway (PPP) is another way to provide for the tumor cell, which is related to a shift in ATP production from mitochondrial OXPHOS to substrate-level phosphorylation (Skolik et al., 2021). In the PPP, Glucose-6-phosphate dehydrogenase (G6PD) is the main enzyme that catalyzes the first reaction, providing reducing power to all cells in the form of NADPH (Patra and Hay, 2014). Therefore, the damage of G6PD may hinder or slow the energy supply through glycolysis. Our study demonstrates a shift in the fraction of total ATP production in HepG2 cells exposed to the middle concentration of AFB1, and a significant shift in cells exposed to all high concentrations of MIX. It is hypothesized that AFB1 may reduce the activity of G6PD enzyme, inhibiting glycolysis from producing ATP and leading to this shift in ATP production in HepG2 cells. Previous study by Raafat et al. have reported that AFB1 exposure is associated with an evident decline in the activity of the G6PD enzyme (Raafat et al., 2021). In addition, Liu et al. also mentioned that there might be a novel association of G6PD activity with AFB1-related xenobiotic metabolism (Lin et al., 2013). These previous studies could support our conjecture that AFB1 may reduce the G6PD activity. Our previous studies on the microbial toxin called cereulide, a *Bacillus cereus* emetic toxin, revealed that it induces toxicity in HepG2 cells by impairing mitochondrial function. Oxygen consumption rate analyses and bioenergetics assessment using the Seahorse XF analyzer showed a measurable mitochondrial impairment at doses of cereulide lower than the AFB1 and FB1 concentrations used in this study, as evidenced by a reduction in maximal cell respiration.

When considering the specific glycolytic and mitochondrial parameters separately, it was observed that AFB1, FB1, and MIX could significantly inhibit ATP production in both pathways in HepG2 cells. Especially upon exposure to high mycotoxin concentrations, the MIX of AFB1 and FB1 showed a significant decrease in all mitochondrial parameters in HepG2 cells compared to only AFB1/ FB1. In contrast, no significance in glycolysis parameters was observed between MIX and single treatments. The decrease in the ATP-linked OCR suggests a low ATP demand, lack of substrate availability, and/or severe damage to OXPHOS. The remaining rate of mitochondrial respiration, defined as proton leak, consists of protons transported through the mitochondrial membrane during electron transport, which results in oxygen consumption but not ATP production. The spare respiratory capacity (SRC), which characterizes the mitochondrial ability to meet additional energy requirements beyond the basal level in response to acute cellular stress or heavy workload, thereby avoiding an ATP crisis, can be viewed as a determination of mitochondrial fitness, a reflection of “healthy” mitochondria (Marchetti et al., 2020). When cells are stressed, the energy demand increases, with more ATP required to maintain cellular functions (Yamamoto et al., 2016). Our results demonstrated that the combination of AFB1 and FB1 likely caused to a significant interaction, resulting in more disruption of the mitochondrial metabolism and apoptosis involving Complexes I-V. As a mode of action, AFB1 exposure can also cause hepatotoxicity at the DNA level, accompanied by several metabolic changes, including cell membrane metabolism, glycolysis, and TCA cycle functioning, mainly cause oxidative-stress-mediated impairments of mitochondria functions (Zhang et al., 2011; Zhou et al., 2021).

In line with previous research, AFB1 impairs mitochondrial respiration, causes MMP loss, reduces ATP content, and inhibits the function of mitochondrial complexes I-IV (Chen et al., 2022; Xu et al., 2021). Similarly, FB1 is involved in mitochondrial dysfunction by inhibiting ETC in mitochondrial respiration (Chen et al., 2022; Sheik Abdul and Marnewick, 2020). Therefore, AFB1 and FB1 could disrupt mitochondrial respiration by inhibiting ETC, which could be why the mixture of AFB1 and FB1 worsened the mitochondrial dysfunction and showed a significant interaction in the disruption of mitochondrial metabolism. Impaired ETC due to compromised mitochondrial respiration may emit additional p53 induction with consequent cellular damage (Khutornenko et al., 2010). According to the transcriptomic results obtained from our study and previous literature reports, it seems that AFB1 and FB1 increase the expression of p53. This could be another contributing factor to the significant interaction observed between AFB1 and FB1 in causing damage to the mitochondria (Cao et al., 2022; Molina-Pintor et al., 2022).

4.3. Transcriptomics reveals interactions between AFB1 and FB1 at the level of mitochondrial functioning and apoptosis

Metabolic flux measurements from the Seahorse assays and RNA sequencing analysis of AFB1, FB1, and MIX in HepG2 cells indicated modes of action related to cell death, apoptosis, or mitochondrial dysfunction. Interestingly, the MIX (AFB1 and FB1) has more similar DEGs with FB1 than with AFB1, suggesting that FB1 may dictate the

combined response more than AFB1. Nonetheless, the MIX upregulated 72 DEGs (including CPLX2, DDX46, ABCC11, SARDH, and CYP24A1 genes, related to mitochondrial metabolism) and downregulated 10 DEGs (including RFX2 gene, a DNA-binding protein and CD274 gene, indirectly involved in programmed cell death). These results suggest that AFB1 and FB1 may co-regulate the expression of some genes, resulting in a significant interaction. Our findings also showed that the p53 pathway is one of the co-regulated signaling pathways by AFB1 and FB1, and is associated with mitochondrial dysfunction resulting in apoptosis. The p53 pathway plays a critical role in regulating cellular responses to various stress types, including mitochondrial apoptosis, DNA repair, and genetic stability. Additionally, it can directly participate in intrinsic apoptosis by interacting with the Bcl-2 family to induce mitochondrial dysfunction (Vaseva and Moll, 2009). This system is essential in humans for genome integrity, DNA repair, and apoptosis (Bernstein et al., 2002).

During apoptosis, the stabilization and activation of p53 lead to programmed cell death (Yu et al., 2009). Therefore, p53 regulates proteins, such as cell surface death receptors proteins (Fas/APO1 and KILLER/DR5), cytoplasmic pro-apoptotic proteins (PIDD and Bid), and mitochondrial pro-apoptotic proteins (Bax, Bak, PUMA, and NOXA) (Burns and El-Deiry, 1999; Oda et al., 2000; Sax and El-Deiry, 2003; Wei et al., 2001; Yu et al., 2003). In the current study, Fas, DR5, PUMA, Noxa, and PIGs genes were significantly downregulated by the MIX group (AFB1 and FB1) compared to single FB1 exposure, which could be associated with mitochondrial dysfunction. It also was found that the MIX significantly upregulated the p53 gene and downregulated Cx I, Cx II, Cx III, and Cx IV genes in the p53 signaling pathway, which could explain the significant interaction between AFB1 and FB1 on mitochondrial damage. This obtained damage would impair the ETC, leading to an additional emit of p53 (Khutornenko et al., 2010). It has also been reported that inhibiting the mitochondrial cytochrome bc1 (the ETC complex III) could induce a strong p53 response and p53 accumulation, which is associated with mitochondrial depolarization and mitochondrial complex IV inactivity (Marchenko and Moll, 2014). The study by Saleem et al. also mentioned that lower complex IV activity and several impaired indexes of mitochondrial function are related to p53 (Saleem et al., 2015). AFB1 and FB1 individually affected the p53 and complexes, which could be the reason for the significant inhibition on mitochondrial respiration in the MIX upon the significant upregulation of p53 gene and downregulation of Cx I, Cx II, Cx III, and Cx IV genes. As reported in the literature, HepG2 cells exposed to either AFB1 or FB1 showed a higher abundance of p53 (Budin et al., 2021; Li et al., 2021). Moreover, Du et al. demonstrated that when AFB1 and FB1 were combined, a higher optical density of p53 was observed by immunohistochemical analysis, and they hypothesized that there could be an interaction between AFB1 and FB1 in inducing HepG2 cell apoptosis (Du et al., 2017). Similarly, in our current study, MIX exposure resulted in a significant upregulation of p53, supporting the notion that AFB1 and FB1 can interact to induce HepG2 cell apoptosis. The pattern of p53-induced gene expression can lead to apoptosis by regulating certain proteins. The activity of the p53 protein, as a transcription factor, is highly regulated, and its basal activity is greatly enhanced in cells exposed to a wide variety of stress signals, allowing it to activate the apoptotic pathway (Lane and Lain, 2002). In the apoptosis pathway, the p53 protein directly interacts with the multidomain members of the Bcl-2 family, inducing mitochondrial outer membrane permeabilization (Marchenko and Moll, 2014). The exposure to the MIX (AFB1 and FB1) significantly activated the p53, suggesting that it could play a central role in the interconnections between signal transduction pathways.

It has been verified that AFB1 inhibits mitochondrial complex I-IV activities, and FB1 inhibits mitochondrial complex I by decreasing complex sphingolipids (Huang et al., 2020). This is also in line with our findings, where the MIX significantly downregulated Cx I, Cx II, Cx III, and Cx IV genes. These genes are central mitochondria respiratory complexes in the ETC and linked to cytochrome *c* (CytC), which induces apoptosis in the p53 pathway. CytC is released into the cytosol where the protein binds to Apaf-1, activates CASP9, and triggers an enzymatic cascade leading to cell death (Schuler et al., 2000). In our study, the expression of CytC, Apaf-1, CASP9, and CASP3 genes was decreased by the exposure to the MIX compared to the exposure to FB1. The release of CytC from mitochondria is a major event in the death receptor-independent, "intrinsic," apoptotic pathway (Desagher and Martinou, 2000). CytC is essential for the assembly and respiratory function of the enzyme complex. The lack of CytC decreases the stability of complex IV, reduces electron transport complex III activity, and modifies redox metabolism (Welchen et al., 2012). CytC, along with ATP and Apaf-1, facilitates activation by CASP9 of the effector caspases CASP3 (Slee et al., 1999), which cleave their substrates and lead to apoptotic cell death. This complex of CytC, Apaf-1, and CASP9 is commonly referred to as the apoptosome (Bratton et al., 2001). The reduced form of CytC also binds less to anions and binds less tightly to negatively charged membranes. This could be the reason for a significant interaction between AFB1 and FB1 on mitochondrial dysfunction and HepG2 cell apoptosis by disrupting the mitochondrial complexes and CytC in the p53 pathway.

DNA repair is another system in the p53 pathway. The stabilization and activation of p53 lead to cell cycle arrest by increasing GADD45 (Jin et al., 2002) and initiating DNA repair through p53R2 and p48 (Tanaka et al., 2000). Cells that are defective in DNA repair tend to accumulate excess DNA damage. In addition, cells that are defective in apoptosis tend to survive even with DNA damage, and the subsequent DNA replication during cell division may cause persistent mutations leading to carcinogenesis (Bernstein et al., 2002). Usually, DNA damage is repaired by base excision repair (BER) by mitochondrial enzymes. Mitochondrial DNA comprises 0.1–1.0% of the total DNA in most mammalian cells (Singh et al., 1992). Mitochondrial DNA has been proposed to be involved in carcinogenesis because of its high susceptibility to mutations and limited repair mechanisms compared to genomic DNA (Penta et al., 2001). If the mitochondrial DNA damage cannot be repaired, it leads to disruption of the ETC and mitochondrial dysfunction (Mandavilli et al., 2002). In general, the energy-demanding process of DNA repair requires proper utilization of the available ATP in the cell, which is provided by the mitochondria (Bernstein et al., 2002). Therefore, mitochondrial DNA repair plays a central role in maintaining (energy) homeostasis in the cell. In our study, P48, p53R2, Gadd45, and Sestrins genes were significantly downregulated by the MIX (ABF1 and FB1) compared to the individual FB1 treatment in HepG2 cells. This suggests that the combination of AFB1 and FB1 could have a significant inhibition interaction on the DNA repair system and, thus, cell homeostasis.

Our study also demonstrates that AFB1, FB1, and their MIX disrupted HepG2 cell proliferation through E2F targets, G2M checkpoint, mitotic spindle, MYC targets, and p53 pathway. Deregulated cell proliferation could propel the tumor cell and its progeny into uncontrolled expansion and invasion beneath the complexity and idiopathy of every cancer. Neoplastic progression may be further facilitated by the deregulated cell proliferation that, along with the necessary compensatory suppression of apoptosis, supports it (Evan and Vousden, 2001). Previous studies illustrated that individual exposure to AFB1 or FB1 could inhibit cell proliferation to increase apoptosis (Singh and Kang, 2017; Zhou et al., 2019). Therefore, combining AFB1 and FB1 may deregulate proliferation, triggering apoptosis.

5. Conclusion

The effect of AFB1 and FB1 on HepG2 cells has been examined regarding their cytotoxicity endpoints (cell viability, ROS generation, and MMP disruption), total ATP production, glycolytic, mitochondrial function, and gene expression in the cell apoptosis process. The combined exposure of both mycotoxins induced a more inhibitory effect on cellular viability and caused an increase in ROS production, and

disruption of MMP. Respirometry and transcriptomics demonstrated a significant interaction between AFB1 and FB1 in mitochondrial dysfunction and apoptosis pathways, most probably triggered by the p53 pathway and mitochondrial complex Cx I-IV genes. In addition, AFB1 and FB1 affected DNA repair and induced cell proliferation in HepG2 cells in a possible synergistic way as they have different targets in cell apoptosis. Indeed, testing the effect of long-term of exposure at low doses of AFB1 and FB1 is required to have a better understanding on their chronic toxicity. Furthermore, the implementation of the recent techniques of 3D liver culture systems (spheroids and organoids) will be more appropriate to assess the toxic mechanism of AFB1, FB1 and their binary mixture as these systems express more relevant physiological and tissue-specific characteristics, resembling *in vivo* complex architecture, microenvironment, and cellular functions.

Funding

This work was conducted within the Horizon 2020 IMPTOX project (https://www.imptox.eu), funded by the European Union's Horizon 2020 research and innovation program under the grant agreement No 965173, Research Foundation Flanders research grant 1506419N given to AR, Ghent University Special Research Fund grant given BOF20/BAS/120 to AR for the purchase of Seahorse XF analyzer.

CRediT authorship contribution statement

Xiangrong Chen: Conceptualization, Methodology, Validation, Formal analysis, Investigation, Resources, Data curation, Writing – original draft. **Mohamed F. Abdallah:** Formal analysis, Data curation, Writing – review & editing. **Charlotte Grootaert:** Conceptualization, Validation, Data curation, Writing – review & editing. **Filip Van Nieuwerburgh:** Data curation, Methodology, Writing – review & editing. **Andreja Rajkovic:** Conceptualization, Methodology, Project administration, Funding acquisition, Writing – review & editing, Supervision.

Declaration of Competing Interest

The authors declare that they have no known competing financial interests or personal relationships that could have appeared to influence the work reported in this paper.

Data availability

Data will be made available on request.

Acknowledgments

The authors thank China Scholarship Council (CSC) for providing X. C. with a Ph.D. scholarship (File No. 201806170042) to study at Ghent University, Belgium. M.F.A is supported by the Ghent University Special Research Fund (BOF) postdoc mandate with grant number BOF20/PDO/032. The authors thank Ghent University and their respective Faculties and Departments for teamwork, support, and general infrastructure.

***Data** availability*

All data generated or analyzed relevant to the results presented are included in this article.

Aflatoxin B1 (AFB1) and fumonisin B1 (FB1) are two mycotoxins that frequently (co-)contaminate maize. Both toxins are known for their hepatotoxicity in humans. However, their combined toxicity still needs to be investigated, especially for their effect on mitochondria. In this study, the effect of the co-exposure on HepG2 cells was found to be more toxic than the exposure to a single toxin. This due to a significant interaction in mitochondrial dysfunction and apoptosis pathways. This interaction is triggered by the p53 pathway and mitochondrial complex Cx I-IV genes, which promised a new insight into hazardous materials-induced hepatic damage.

References

Abdul, N.S., Chuturgoon, A.A., 2021. Fumonisin B1 regulates LDL receptor and ABCA1 expression in an LXR dependent mechanism in liver (HepG2) cells. Toxicon 190, 58–64. https://doi.org/10.1016/j.toxicon.2020.12.011.

Alam, S., Nisa, S., Daud, S., 2022. Mycotoxins in Environment and Its Health Implications. Springer, Cham, pp. 289–318. https://doi.org/10.1007/978-3-030-96523-5_12.

Bernstein, C., Bernstein, H., Payne, C.M., Garewal, H., 2002. DNA repair/pro-apoptotic dual-role proteins in five major DNA repair pathways: Fail-safe protection against carcinogenesis. Mutation Res. – Rev. Mutation Res. https://doi.org/10.1016/S1383-5742(02)00009-1.

Bratton, S.B., Walker, G., Srinivasula, S.M., Sun, X.M., Butterworth, M., Alnemri, E.S., Cohen, G.M., 2001. Recruitment, activation and retention of caspases-9 and-3 by Apaf-1 apoptosome and associated XIAP complexes. EMBO J. 20, 998–1009. https://doi.org/10.1093/emboj/20.5.998.

Budin, C., Man, H.Y., Al-Ayoubi, C., Puel, S., van Vugt-Lussenburg, B.M.A., Brouwer, A., Oswald, I.P., van der Burg, B., Soler, L., 2021. Versicolorin A enhances the genotoxicity of aflatoxin B1 in human liver cells by inducing the transactivation of the Ah-receptor. Food Chem. Toxicol. 153, 112258 https://doi.org/10.1016/j.fct.2021.112258.

Burns, T.F., El-Deiry, W.S., 1999. The p53 pathway and apoptosis. J. Cell. Physiol. https://doi.org/10.1002/(SICI)1097-4652(199911)181:2<231::AID-JCP5>3.0.CO;2-L.

Cao, W., Yu, P., Yang, K.P., Cao, D., 2022. Aflatoxin B1: metabolism, toxicology, and its involvement in oxidative stress and cancer development. Toxicol. Mech. Methods. https://doi.org/10.1080/15376516.2021.2021339.

Chen, X., Abdallah, M.F., Grootaert, C., Rajkovic, A., 2022. Bioenergetic Status of the Intestinal and Hepatic Cells after Short Term Exposure to Fumonisin B1 and Aflatoxin B1. Int. J. Mol. Sci. 23, 6945. https://doi.org/10.3390/ijms23136945.

Chen, X., Landschoot, S., Detavernier, C., De Saeger, S., Rajkovic, A., Audenaert, K., 2021. Cross-talk between Fusarium verticillioides and Aspergillus flavus in vitro and in planta. Mycotoxin Res. 37, 229–240. https://doi.org/10.1007/s12550-021-00435-x.

Decleer, M., Jovanovic, J., Vakula, A., Udovicki, B., Agoua, R.S.E.K., Madder, A., De Saeger, S., Rajkovic, A., 2018. Oxygen consumption rate analysis of mitochondrial dysfunction caused by bacillus cereus cereulide in Caco-2 and hepG2 cells. Toxins 10, 266. https://doi.org/10.3390/toxins10070266.

Degroote, H., Lefere, S., Vandierendonck, A., Vanderborght, B., Meese, T., Nieuwerburgh, F.V., Verhelst, X., Geerts, A., Vlierberghe, H.V., Devisscher, L., 2021. Characterization of the inflammatory microenvironment and hepatic macrophage subsets in experimental hepatocellular carcinoma models. Oncotarget 12, 562–577. https://doi.org/10.18632/ONCOTARGET.27906.

Desagher, S., Martinou, J.C., 2000. Mitochondria as the central control point of apoptosis. Trends Cell Biol. https://doi.org/10.1016/S0962-8924(00)01803-1.

Du, M., Liu, Y., Zhang, G., 2017. Interaction of aflatoxin B1 and fumonisin B1 in HepG2 cell apoptosis. Food Biosci. 20, 131–140. https://doi.org/10.1016/j.fbio.2017.09.003.

Evan, G.I., Vousden, K.H., 2001. Proliferation, cell cycle and apoptosis in cancer. Nature. https://doi.org/10.1038/35077213.

Feissner, R.F., Skalska, J., Gaum, W.E., Sheu, S.S., 2009. Crosstalk signaling between mitochondrial Ca2+ and ROS. Front. Biosci. 14, 1197–1218. https://doi.org/10.2741/3303.

Fox, C.J., Hammerman, P.S., Thompson, C.B., 2005. Fuel feeds function: Energy metabolism and the T-cell response. Nat. Rev. Immunol. https://doi.org/10.1038/nri1710.

Huang, W., Cao, Z., Yao, Q., Ji, Q., Zhang, J., Li, Y., 2020. Mitochondrial damage are involved in Aflatoxin B1-induced testicular damage and spermatogenesis disorder in mice. Sci. Total Environ. 701, 135077 https://doi.org/10.1016/j.scitotenv.2019.135077.

IARC, 2012. Aflatoxin: Scientific Background, Control, and Implications - Google Books [WWW Document]. IARC (International Agency for Research on Cancer).

Jin, S., Tong, T., Fan, W., Fan, F., Antinore, M.J., Zhu, X., Mazzacurati, L., Li, X., Petrik, K.L., Rajasekaran, B., Wu, M., Zhan, Q., 2002. GADD45-induced cell cycle G2-M arrest associates with altered subcellular distribution of cyclin B1 and is independent of p38 kinase activity. Oncogene 21, 8696–8704. https://doi.org/10.1038/sj.onc.1206034.

Khutornenko, A.A., Roudko, V. V., Chernyak, B. V., Vartapetian, A.B., Chumakov, P.M., Evstafieva, A.G., 2010. Pyrimidine biosynthesis links mitochondrial respiration to the p53 pathway. Proceedings of the National Academy of Sciences of the United States of America 107, 12828–12833. https://doi.org/10.1073/pnas.0910885107.

Lane, D.P., Lain, S., 2002. Therapeutic exploitation of the p53 pathway. Trends Mol. Med. https://doi.org/10.1016/S1471-4914(02)02309-2.

Li, C., Liu, X., Wu, J., Ji, X., Xu, Q., 2022. Research progress in toxicological effects and mechanism of aflatoxin B1 toxin. PeerJ 10. https://doi.org/10.7717/peerj.13850.

Li, Q., Yuan, Q., Wang, T., Zhan, Y., Yang, L., Fan, Y., Lei, H., Su, J., 2021. Fumonisin B1 inhibits cell proliferation and decreases barrier function of swine umbilical vein endothelial cells. Toxins 13. https://doi.org/10.3390/toxins13120863.

Lin, H.R., Wu, C.C., Wu, Y.H., Hsu, C.W., Cheng, M.L., Chiu, D.T.Y., 2013. Proteome-wide dysregulation by glucose-6-phosphate dehydrogenase (G6PD) reveals a novel protective role for G6PD in aflatoxin B1-mediated cytotoxicity. J. Proteome Res. 12, 3434–3448. https://doi.org/10.1021/pr4002959.

Mandavilli, B.S., Santos, J.H., Van Houten, B., 2002. Mitochondrial DNA repair and aging. Mutation Res. – Fundam. Mol. Mech. Mutagenesis 509, 127–151. https://doi.org/10.1016/S0027-5107(02)00220-8.

Marchenko, N.D., Moll, U.M., 2014. Mitochondrial death functions of p53. Mol. Cell. Oncol. https://doi.org/10.1080/23723548.2014.955995.

Marchetti, P., Fovez, Q., Germain, N., Khamari, R., Kluza, J., 2020. Mitochondrial spare respiratory capacity: Mechanisms, regulation, and significance in non-transformed and cancer cells. FASEB J. https://doi.org/10.1096/fj.202000767R.

Marusyk, A., Polyak, K., 2010. Tumor heterogeneity: Causes and consequences. Biochimica et Biophysica Acta - Reviews on Cancer. https://doi.org/10.1016/j.bbcan.2009.11.002.

Meneely, J.P., Hajšlová, J., Krska, R., Elliott, C.T., 2018. Assessing the combined toxicity of the natural toxins, aflatoxin B1, fumonisin B1 and microcystin-LR by high content analysis. Food Chem. Toxicol. 121, 527–540. https://doi.org/10.1016/j.fct.2018.09.052.

Molina-Pintor, I.B., Rojas-García, A.E., Medina-Díaz, I.M., Barrón-Vivanco, B.S., Bernal-Hernández, Y.Y., Ortega-Cervantes, L., Ramos, A.J., Herrera-Moreno, J.F., González-Arias, C.A., 2022. An update on genotoxic and epigenetic studies of fumonisin B 1. World Mycotoxin J. 15, 57–72. https://doi.org/10.3920/wmj2021.2720.

Oda, E., Ohki, R., Murasawa, H., Nemoto, J., Shibue, T., Yamashita, T., Tokino, T., Taniguchi, T., Tanaka, N., 2000. Noxa, a BH3-only member of the Bcl-2 family and candidate mediator of p53-induced apoptosis. Science 288, 1053–1058. https://doi.org/10.1126/science.288.5468.1053.

Palumbo, R., Crisci, A., Venâncio, A., Abrahantes, J.C., Dorne, J.L., Battilani, P., Toscano, P., 2020. Occurrence and co-occurrence of mycotoxins in cereal-based feed and food. Microorganisms 8, 74. https://doi.org/10.3390/microorganisms8010074.

Patra, K.C., Hay, N., 2014. The pentose phosphate pathway and cancer. Trends Biochem. Sci. https://doi.org/10.1016/j.tibs.2014.06.005.

Penta, J.S., Johnson, F.M., Wachsman, J.T., Copeland, W.C., 2001. Mitochondrial DNA in human malignancy. Mutation Res. – Rev. Mutation Res. https://doi.org/10.1016/S1383-5742(01)00053-9.

Prakash, C., Chhikara, S., Kumar, V., 2022. Mitochondrial Dysfunction in Arsenic-Induced Hepatotoxicity: Pathogenic and Therapeutic Implications. Biol. Trace Elem. Res. https://doi.org/10.1007/s12011-021-02624-2.

Raafat, N., Emam, W.A., Gharib, A.F., Nafea, O.E., Zakaria, M., 2021. Assessment of serum aflatoxin B1 levels in neonatal jaundice with glucose-6-phosphate dehydrogenase deficiency: a preliminary study. Mycotoxin Res. 37, 109–116. https://doi.org/10.1007/s12550-020-00421-9.

Saleem, A., Iqbal, S., Zhang, Y., Hood, D.A., 2015. Effect of p53 on mitochondrial morphology, import, and assembly in skeletal muscle. American Journal of Physiology - Cell Physiology 308, C319–C329. https://doi.org/10.1152/ajpcell.00253.2014.

Sax, J.K., El-Deiry, W.S., 2003. p53 downstream targets and chemosensitivity. Cell Death Differ. https://doi.org/10.1038/sj.cdd.4401227.

Schuler, M., Bossy-Wetzel, E., Goldstein, J.C., Fitzgerald, P., Green, D.R., 2000. p53 induces apoptosis by caspase activation through mitochondrial cytochrome c release. J. Biol. Chem. 275, 7337–7342. https://doi.org/10.1074/jbc.275.10.7337.

Sheik Abdul, N., Marnewick, J.L., 2020. Fumonisin B1-induced mitochondrial toxicity and hepatoprotective potential of rooibos: An update. J. Appl. Toxicol. https://doi.org/10.1002/jat.4036.

Singh, G., Sharkey, S.M., Moorehead, R., 1992. Mitochondrial DNA damage by anticancer agents. Pharmacol. Ther. https://doi.org/10.1016/0163-7258(92)90033-V.

Singh, M.P., Kang, S.C., 2017. Endoplasmic reticulum stress-mediated autophagy activation attenuates fumonisin B1 induced hepatotoxicity in vitro and in vivo. Food Chem. Toxicol. 110, 371–382. https://doi.org/10.1016/j.fct.2017.10.054.

Singto, T., Tassaneeyakul, W., Porasuphatana, S., 2020. Protective effects of purple waxy corn on aflatoxin B1-induced oxidative stress and micronucleus in HepG2 cells. Indian J. Pharm. Sci. 82, 506–513. https://doi.org/10.36468/pharmaceutical-sciences.674.

Skolik, R.A., Solocinski, J., Konkle, M.E., Chakraborty, N., Menze, M.A., 2021. Global changes to HepG2 cell metabolism in response to galactose treatment. American Journal of Physiology - Cell Physiology 320, C778–C793. https://doi.org/10.1152/ajpcell.00460.2020.

Slee, E.A., Harte, M.T., Kluck, R.M., Wolf, B.B., Casiano, C.A., Newmeyer, D.D., Wang, H. G., Reed, J.C., Nicholson, D.W., Alnemri, E.S., Green, D.R., Martin, S.J., 1999. Ordering the cytochrome c-initiated caspase cascade: Hierarchical activation of caspases-2,-3,-6,-7,-8, and -10 in a caspase-9-dependent manner. J. Cell Biol. 144, 281–292. https://doi.org/10.1083/jcb.144.2.281.

Tanaka, H., Arakawa, H., Yamaguchi, T., Shiraishi, K., Fukuda, S., Matsui, K., Takei, Y., Nakamura, Y., 2000. A ribonucleotide reductase gene involved in a p53-dependent cell-cycle checkpoint for DNA damage. Nature 404, 42–49. https://doi.org/10.1038/35003506.

Vaseva, A.V., Moll, U.M., 2009. The mitochondrial p53 pathway. Biochim. Biophys. Acta Bioenerg. 1787, 414–420. https://doi.org/10.1016/j.bbabio.2008.10.005.

Vyas, S., Zaganjor, E., Haigis, M.C., 2016. Mitochondria and Cancer. Cell. https://doi.org/10.1016/j.cell.2016.07.002.

Wang, Y., Liu, F., Zhou, X., Liu, M., Zang, H., Liu, X., Shan, A., Feng, X., 2022. Alleviation of Oral Exposure to Aflatoxin B1-Induced Renal Dysfunction, Oxidative Stress, and Cell Apoptosis in Mice Kidney by Curcumin. Antioxidants 11, 1082. https://doi.org/10.3390/antiox11061082.

Wei, M.C., Zong, W.X., Cheng, E.H.Y., Lindsten, T., Panoutsakopoulou, V., Ross, A.J., Roth, K.A., Macgregor, G.R., Thompson, C.B., Korsmeyer, S.J., 2001. Proapoptotic BAX and BAK: A requisite gateway to mitochondrial dysfunction and death. Science 292, 727–730. https://doi.org/10.1126/science.1059108.

Welchen, E., Hildebrandt, T.M., Lewejohann, D., Gonzalez, D.H., Braun, H.P., 2012. Lack of cytochrome c in Arabidopsis decreases stability of Complex IV and modifies redox metabolism without affecting Complexes I and III. Biochim. Biophys. Acta Bioenerg. 1817, 990–1001. https://doi.org/10.1016/j.bbabio.2012.04.008.

Wu, F., Groopman, J.D., Pestka, J.J., 2014. Public health impacts of foodborne mycotoxins. Annu. Rev. Food Sci. Technol. 5, 351–372. https://doi.org/10.1146/annurev-food-030713-092431.

Xu, F., Li, Y., Cao, Z., Zhang, J., Huang, W., 2021. AFB1-induced mice liver injury involves mitochondrial dysfunction mediated by mitochondrial biogenesis inhibition. Ecotoxicol. Environ. Saf. 216, 112213 https://doi.org/10.1016/j.ecoenv.2021.112213.

Yamamoto, H., Morino, K., Mengistu, L., Ishibashi, T., Kiriyama, K., Ikami, T., Maegawa, H., 2016. Amla Enhances Mitochondrial Spare Respiratory Capacity by Increasing Mitochondrial Biogenesis and Antioxidant Systems in a Murine Skeletal Muscle Cell Line. Oxid. Med. Cell. Longev. 2016 https://doi.org/10.1155/2016/1735841.

Yu, J., Wang, Z., Kinzler, K.W., Vogelstein, B., Zhang, L., 2003. PUMA mediates the apoptotic response to p53 in colorectal cancer cells. Proceedings of the National Academy of Sciences of the United States of America 100, 1931–1936. https://doi.org/10.1073/pnas.2627984100.

Yu, Z., Wang, H., Zhang, L., Tang, A., Zhai, Q., Wen, J., Yao, L., Li, P., 2009. Both p53-PUMA/NOXA-Bax-mitochondrion and p53–p21cip1 pathways are involved in the CDglyTK-mediated tumor cell suppression. Biochem. Biophys. Res. Commun. 386, 607–611. https://doi.org/10.1016/j.bbrc.2009.06.083.

Zhang, L., Ye, Y., An, Y., Tian, Y., Wang, Y., Tang, H., 2011. Systems responses of rats to aflatoxin B1 exposure revealed with metabonomic changes in multiple biological matrices. J. Proteome Res. 10, 614–623. https://doi.org/10.1021/pr100792q.

Zheng, J., 2012. Energy metabolism of cancer: Glycolysis versus oxidative phosphorylation (review). Oncol. Lett. https://doi.org/10.3892/ol.2012.928.

Zhou, J., Tang, L., Wang, J.S., 2021. Aflatoxin B1Induces Gut-Inflammation-Associated Fecal Lipidome Changes in F344 Rats. Toxicol. Sci. 183, 363–377. https://doi.org/10.1093/toxsci/kfab096.

Zhou, R., Liu, M., Liang, X., Su, M., Li, R., 2019. Clinical features of aflatoxin B1-exposed patients with liver cancer and the molecular mechanism of aflatoxin B1 on liver cancer cells. Environ. Toxicol. Pharmacol. 71, 103225 https://doi.org/10.1016/j.etap.2019.103225.

Zhu, Q., Ma, Y., Liang, J., Wei, Z., Li, M., Zhang, Y., Liu, M., He, H., Qu, C., Cai, J., Wang, X., Zeng, Y., Jiao, Y., 2021. AHR mediates the aflatoxin B1 toxicity associated with hepatocellular carcinoma. Signal Transduct. Target. Ther. 6, 1–13. https://doi.org/10.1038/s41392-021-00713-1.

Zorova, L.D., Popkov, V.A., Plotnikov, E.Y., Silachev, D.N., Pevzner, I.B., Jankauskas, S. S., Babenko, V.A., Zorov, S.D., Balakireva, A.V., Juhaszova, M., Sollott, S.J., Zorov, D.B., 2018. Mitochondrial membrane potential. Anal. Biochem. 552, 50–59. https://doi.org/10.1016/j.ab.2017.07.009.

Zu, X.L., Guppy, M., 2004. Cancer metabolism: Facts, fantasy, and fiction. Biochem. Biophys. Res. Commun. https://doi.org/10.1016/j.bbrc.2003.11.136.